INFECTION AND IMMUNITY, Nov. 2009, p. 4771–4782 Vol. 77, No. 11
0019-9567/09/$12.00 doi:10.1128/IAI.00850-09

Yersinia pseudotuberculosis Virulence Determinants Invasin, YopE, and YopT Modulate RhoG Activity and Localization▽

Sina Mohammadi[2] and Ralph R. Isberg[1,2]*

Howard Hughes Medical Institute[1] and Department of Molecular Biology and Microbiology,[2] Tufts University School of Medicine, Boston, Massachusetts 02111

Received 28 July 2009/Returned for modification 20 August 2009/Accepted 25 August 2009

The *Yersinia pseudotuberculosis* surface protein invasin binds to multiple β1 integrins with high affinity, leading to misregulation of Rac1 activity. Upon host cell binding, alteration of Rho GTPase activity results from the action of several *Yersinia* outer proteins (Yops) that are translocated into the cytoplasm. We report here that three virulence determinants encoded by *Y. pseudotuberculosis* manipulate the Rho GTPase RhoG. *Y. pseudotuberculosis* binding to cells caused robust recruitment of RhoG to the site of attachment, which required high-affinity invasin-β1 integrin association. Furthermore, inactivation of RhoG significantly reduced the efficiency of invasin-mediated bacterial internalization. To investigate the activation state of RhoG, a fluorescence resonance energy transfer-based activation biosensor was developed and used to show distinct spatial activation of RhoG at the site of bacterial attachment. The biosensor was also used to show efficient RhoG inactivation by *Y. pseudotuberculosis* YopE, a potent Rho GTPase activating protein. Additionally, RhoG mislocalization by the prenylcysteine endoprotease YopT was demonstrated by two independent assays. Functional bacterial uptake experiments demonstrated that RhoG activation can bypass a deficit in Rac1 activity. Interestingly, increasing the size of the particle gave results more consistent with a linear pathway, in which RhoG acts as an upstream activator of Rac1, indicating that increased surface area introduces constraints on the signaling pathways required for efficient internalization. Taken together, these data demonstrate the misregulation of RhoG by multiple *Y. pseudotuberculosis* virulence determinants. Since RhoG is imperative for proper neutrophil function, this misregulation may represent a unique mechanism by which *Yersinia* species dampen the immune response.

The enteropathogens *Yersinia pseudotuberculosis* and *Yersinia enterocolitica* gain access to the intestinal lymphatic system by traversing the M-cell layer and invading Peyer's patches (2, 39). This infiltration requires the bacterial cell surface protein invasin (32). *Y. pseudotuberculosis* invasin binds to at least five β1 integrins (cell adhesion receptors [23]) and mediates tight interaction with host cells (25). This tight binding leads to the activation of the receptor, generating a robust signal, which leads to the internalization of the bacterium (13, 24). A number of signaling molecules are required for this internalization event, including the Rho family GTPases.

The Rho GTPase family, a subclass of the Ras superfamily of GTPases, control a diverse range of cellular processes such as morphogenesis, migration, cell cycle progression, and cytoskeletal rearrangements (26). Rho family members are small proteins (~21 to 27 kDa) that exist in active (GTP-bound) and inactive (GDP-bound) conformations. In the active conformation, the GTPases interact with a number of downstream effector molecules (26). Regulation of GTPase activity is intricately controlled on three levels. First, activation is carried out by guanine nucleotide exchange factors (GEFs), which exchange GDP for GTP (6, 43). GTP-bound (active) proteins are targeted to membranous structures via C-terminal prenyl moieties that are added posttranslationally to the C-terminal CAAX box (44, 54). The type of membranous structure to which the GTPase localizes is influenced by the region upstream of the CAAX box, commonly referred to as the polybasic region (PBR) (59). Second, when signaling requires termination, the GTPase is inactivated by GTPase activating proteins (GAPs), which enhance intrinsic GTP hydrolysis (49). Third, the GDP-bound (inactive) protein is sequestered in the cytoplasm by guanine nucleotide dissociation inhibitor proteins, which mask the hydrophobic C-terminal lipid moiety (12, 14). Pathogenic *Yersinia* species encode factors that interfere with all three Rho GTPase regulatory mechanisms.

Several of these factors are encoded on the *Yersinia* virulence plasmid, which also encodes a type III secretion system (T3SS) to deliver *Yersinia* outer proteins (Yops) into the host cell cytosol after the establishment of intimate host-pathogen contact (33, 51). These translocated substrates act collectively to keep the bacterium extracellular after passage through the M-cell layer and to dampen immune responses in the host organism (9, 45). Two translocated substrates, YopE and YopT, directly target Rho GTPases.

YopE is a Rho GAP that inactivates Rac1, Cdc42, and RhoA (3, 57), leading to disruption of the actin cytoskeleton, which prevents invasin-mediated internalization of the bacterium and eventually leads to cell rounding. YopT also interferes with the actin cytoskeleton. YopT is a prenylcysteine endoprotease, which cleaves Rac1, Cdc42, and RhoA upstream of the prenylated cysteine residue of the CAAX motif (47), thus removing the GTPases from the plasma membrane. YopE and YopT seem to synergize in order to dampen signals necessary for bacterial internalization (57), thereby

* Corresponding author. Mailing address: 150 Harrison Ave. J424, Boston, MA 02111. Phone: (617) 636-3993. Fax: (617) 636-0337. E-mail: Ralph.Isberg@tufts.edu.

▽ Published ahead of print on 31 August 2009.

TABLE 1. Plasmids and bacterial strains used in this study

Plasmid, protein, or strain	Description	Source or reference
Plasmids and proteins		
EGFP-RhoG(wt)	Wild-type RhoG with N-terminal EGFP tag	This study
EGFP-RhoG(G12V)	GTPase-deficient (constitutively active) RhoG with N-terminal EGFP tag	This study
EGFP-RhoG(T17N)	Dominant-negative RhoG with N-terminal EGFP tag	This study
EGFP-Rac1(wt)	Wild-type Rac1 with N-terminal EGFP tag	This study
pRNAT-Scrambled KD[a]	RNAi plasmid encoding a control (nontargeting) shRNA	This study
pRNAT-RhoG KD	RNAi plasmid encoding a RhoG-targeting shRNA	This study
pRNAT-Rac1 KD	RNAi plasmid encoding a Rac1-targeting shRNA	This study
mCFP-RhoG(wt)[b]	Wild-type RhoG with N-terminal mCFP tag	This study
mCFP-RhoG(G12V)	GTPase-deficient RhoG with N-terminal mCFP tag	This study
mCFP-RhoG(T17N)	Dominant-negative RhoG with N-terminal mCFP tag	This study
mCFP-RhoG(F37A)	Effector binding mutant RhoG with N-terminal mCFP tag	This study
mCFP-RhoG(Y40C)	Effector binding mutant RhoG with N-terminal mCFP tag	This study
ELMO-mYFP	Rat ELMO2(AA1-362) with C-terminal mYFP tag	This study
mCFP-Rac1(wt)	Wild-type Rac1 with N-terminal mCFP tag	57
PBD-mYFP[b]	p21 binding domain from Pak1 with C-terminal mYFP tag	57
myc-mCFP-RhoG(G12V)	GTPase-deficient RhoG with N-terminal myc-mCFP tag	This study
myc-mCFP-Rac1(G12V)	GTPase-deficient Rac1 with N-terminal myc-mCFP tag	This study
Arf6-HA	Wild-type Arf6 with C-terminal HA tag	15
Strains		
YPIII(P^+)	Parental *Y. pseudotuberculosis* strain (naturally *yopT* and *sycT* deficient)	4
YPIII(P^-)	Plasmid-cured *Y. pseudotuberculosis* strain	4
YPIII *yopB*	YPIII(P^+) with in-frame *yopB* deletion	30
YP17	YPIII(P^+) with in-frame *yopE* and *yopH* deletions	3
YP17/pYopE	YP17 with plasmid carrying *yopE* under the control of an inducible promoter	3
YP17/pYopT	YP17 with plasmid carrying *yopT* and *sycT* under the control of the *yopH* promoter	52

[a] KD, knockdown.
[b] mCFP and mYFP, monomeric cyan and yellow fluorescent proteins, respectively.

keeping *Yersinia* in the relative safety of the extracellular milieu.

Potential targeting of other Rho family GTPases by *Y. pseudotuberculosis* is not known. Rac1, Cdc42, and RhoA are the best-studied members of this GTPase family, but *Yersinia* could also target other family members. Of these, RhoG has the closest connections to ligation of β1 integrin receptors (27). This connection is particularly intriguing because *Y. pseudotuberculosis* invasin binds to several β1 integrins. Additionally, a previous study has indicated that the related organism *Y. enterocolitica* can modulate RhoG activity (42). Interestingly, RhoG plays a critical role in proper neutrophil function since it has been shown to be necessary for efficient generation of reactive oxygen species (ROS) by neutrophils (7). Furthermore, pathogenic *Yersinia* species preferentially deliver Yop effectors into neutrophils (31) and inhibit the generation of ROS in that cell type (48). Additionally, neutropenic mice are more susceptible to *Yersinia* infection (8). Taken together, these data suggest that neutrophil inactivation is critical for maintenance of infection. If targeted by Yops, RhoG could represent a molecular target for neutrophil inactivation by *Y. pseudotuberculosis*.

In this study, we performed a detailed investigation of the manipulation of RhoG function by *Y. pseudotuberculosis*. Using a novel fluorescence resonance energy transfer (FRET)-based biosensor, we show local elevation in RhoG activity in response to invasin binding. We also show that RhoG is inactivated by *Y. pseudotuberculosis* YopE and mislocalized by *Y. pseudotuberculosis* YopT. Finally, we demonstrate that requirements for RhoG signaling during phagocytosis are dictated by the size of particle being ingested. These data support a model where modulation of RhoG activity and localization by specific *Y. pseudotuberculosis* virulence determinants lead to successful establishment and maintenance of infection.

MATERIALS AND METHODS

Bacterial and mammalian cell culture. All strains used are summarized in Table 1. *Yersinia pseudotuberculosis* strain YPIII (4, 18, 40) was used in all studies. YPIII is a clinical isolate that naturally lacks *yopT* and its chaperone, *sycT* (52). Unless otherwise indicated, uptake assays were performed with a virulence plasmid-cured strain [YPIII(P^-)]. The strains YP17 [YPIII(P^+) Δ*yopE* Δ*yopH*], YP17/pYopE (3), and YP17/pYopT (50, 52) have been described previously and were kind gifts from J. Bliska (Stony Brook University, Stony Brook, NY). The *yopB*-deficient *Y. pseudotuberculosis* strain has been described previously (30) and was a kind gift from J. Mecsas (Tufts University School of Medicine). The *Y. pseudotuberculosis* strain containing the D911A invasin allele (*invD911A*) has been described previously (29). COS1 (20) and HeLa (19) cells were obtained from ATCC and maintained in Dulbecco's modified Eagle's medium supplemented with 10% heat-inactivated fetal bovine serum.

Plasmids and transfection. All plasmids used in this study are summarized in Table 1. All mammalian cDNA clones used in this study are of human origin, unless otherwise indicated. For fluorescence imaging, RhoG and Rac1 coding sequences were cloned into pEGFP-C1 (Clontech). Plasmids carrying myc-tagged RhoG alleles were kindly provided by H. Katoh (Kyoto University, Kyoto, Japan). A mammalian YopT expression plasmid was constructed by cloning *yopT* from *Y. pseudotuberculosis* IP32953 into p3xFLAG-CMV-7.1 (Sigma). The *yopTC139S* mutant was generated by site-directed mutagenesis. For immunoprecipitation (IP) experiments, coding sequences for constitutively active RhoG with the G12V substitution [RhoG(G12V)] and Rac1(G12V) were cloned into pmyc-mCFP-C1 (58). The plasmid carrying hemagglutinin-tagged Arf6 (Arf6-HA) was kindly provided by C. D'Souza-Schorey (University of Notre Dame, South Bend, IN). Transfections were performed using Lipofectamine 2000 (Invitrogen) according to the manufacturer's recommendations. Typically, cells were transfected for 16 to 20 h, except for RNA interference (RNAi) transfections (see below for details).

***Yersinia* infections and uptake assay.** For uptake assays, plasmid-cured *Yersinia* cells were grown overnight in L broth, back diluted 1:40 in fresh media, and grown to mid-exponential phase (optical density, ≈0.7). Mammalian cells, grown on coverslips, were challenged at a multiplicity of infection (MOI) of ~10 in serum-free media for 30 min. For strains containing the virulence plasmid, overnight cultures were back diluted 1:40 in L broth containing 20 mM $MgCl_2$ and 20 mM sodium oxylate for 2 h at 26°C. Cultures were then shifted to 37°C and grown for an additional 2 h. Inducible promoter expression was triggered by adding 0.5 to 1 mM IPTG (isopropyl-β-D-thiogalactopyranoside) for the last hour of incubation at 37°C. Incubation with mammalian cells was carried out as described above. The cells were fixed with 4% paraformaldehyde in phosphate-buffered saline, and uptake was quantified using an antibody protection assay as described previously (56, 57). Briefly, fixed samples were incubated with anti-*Y. pseudotuberculosis* antibody followed by incubation with a red secondary antibody (Alexa 594 conjugated; Molecular Probes/Invitrogen). Cells were then permeabilized, incubated again with anti-*Y. pseudotuberculosis* antibody, and incubated with a blue secondary antibody (Cascade Blue conjugated; Molecular Probes/Invitrogen). Uptake was quantified by counting the total (blue) and extracellular (pink/red) bacteria per infected cell and calculating the percentage of internalized bacteria. Partially internalized bacteria were scored as extracellular. Typically, ~50 infected cells per coverslip were scored (three coverslips per condition). For localization and FRET assays a higher MOI (~50) was used.

GTPase depletion by RNAi. RhoG and Rac1 were depleted by RNAi, expressed as short hairpin DNA sequences from plasmid pRNAT (GenScript). DNA sequences used were as follows: Nontargeting control (scrambled), AATTCTCCGAACGTGTCACGT; RhoG, AACGCTTTCCCCAAAGAG TAC; Rac1, AAGGAGATTGGTGCTGTAAAA. Multiple RhoG- and Rac1-targeting short hairpin RNAs (shRNAs) were designed and tested; sequences are available upon request. HeLa cells were transfected with shRNA plasmids, and depletion was measured 2 days posttransfection. Quantitative reverse transcription-PCR (RT-PCR) was used to quantify the extent of depletion. Oligonucleotides used for PCR are as follows: RhoG, 5′-CAATGAGGGAG CCACAGAAT-3′ and 5′-GGCACAGAGGAGCAGGTTAG-3′; Rac1, 5′-G GAAGAGAAAATGCCTGCTG-3′ and 5′-GCAAAGCGTACAAAGGTTC C-3′; GAPDH (glyceraldehyde-3-phosphate dehydrogenase), 5′-GATCATC AGCAATGCCTCCT-3′ and 5′-TGTGGTCATGAGTCCTTCCA-3′.

Development of the RhoG FRET biosensor. To develop the FRET biosensors, the RhoG coding sequence was cloned into the pmCFP-C1 plasmid (57). The coding sequence for the N-terminal 362 amino acids of rat ELMO2 (also a kind gift from H. Katoh) were then cloned into pmYFP-N1 (57). This portion of ELMO has been shown to interact specifically with RhoG in a nucleotide-dependent manner (27). Several RhoG alleles were generated to confirm proper interaction patterns. Specifically, G12V, T17N, F37A, and Y40C substitutions in RhoG were generated by site-directed mutagenesis. Plasmids used in FRET experiments are summarized in Table 1. FRET imaging was performed as described previously (57, 58).

FRET images were quantified by analyzing the mean intensity (in arbitrary units) of multiple regions of interest (ROIs) in yellow fluorescent protein (YFP), cyan fluorescent protein (CFP), and FRET images. Sensitized FRET (sFRET) was calculated by subtracting the inherent bleed-through and cross-excitation observed in the FRET filter/cube set. Generally the amount of bleed-through was 0.18 and cross-excitation was 0.32 as described previously (58). Normalized FRET (nFRET) represents the FRET value that is normalized to the expression of the donor and the acceptor and was calculated using the following equation, where I represents mean ROI intensity: $\text{nFRET} = \text{sFRET}/(I_{\text{CFP}} \times I_{\text{YFP}})^{1/2}$.

YopE translocation assay. Translocation was assayed using methods previously described (10). Wild-type [YPIII(P^+)] *Y. pseudotuberculosis* and an isogenic *yopB* mutant were grown overnight in L broth. Cultures were back diluted into high-calcium medium (L broth plus 5 mM $CaCl_2$) and grown at 26°C for 2 h and then at 37°C for 2 h. COS1 cells, grown in six-well dishes, were transfected with either a control or an enhanced green fluorescent protein (EGFP)-RhoG(G12V) construct. Twenty-four hours posttransfection, cells were incubated with wild-type or *yopB* bacteria at an MOI of ~20 for 45 min. Cells were washed with cold phosphate-buffered saline and lysed with eukaryotic lysis buffer (20 mM Tris [pH 7.5], 125 mM NaCl, 1% Nonidet P-40, and protease inhibitor cocktail [Roche]). Lysates were centrifuged at 15,000 × *g* for 15 min to separate the eukaryotic cytosol/translocated materials (supernatant) from bacterial cells and eukaryotic cell debris (pellet). Both fractions were resuspended in sample buffer and analyzed by Western blotting. Fractions were probed for YopE, GFP (Invitrogen), bacterial ribosomal subunit S2, and tubulin (Sigma). Antibodies against YopE and bacterial ribosomal subunit S2 were kind gifts from J. Mecsas (Tufts University School of Medicine). S2 was used to detect the presence of bacteria in the pellet fraction and to detect any contamination from bacterial cytosol into the host cytosol. Tubulin was used as a marker of host cytosol, and GFP was used to detect transfected RhoG(G12V).

YopT cleavage assays. An immunofluorescence-based assay was used to assay YopT targeting of various small GTPases as described previously (57). Briefly, COS1 cells on glass coverslips were transfected overnight with GTPase constructs. Transfected cells were incubated for 30 min with either YP17 or YP17/pYopT and fixed, and bacteria were stained as described above for uptake assays.

Triton X-114 partitioning (22) to assess YopT targeting of Rho GTPases has been described previously (46). Briefly, 293T cells were cotransfected with GTPases (myc-mCFP-RhoG, myc-mCFP-Rac1, and Arf6-HA constructs) and FLAG–wild-type YopT [YopT(wt)] or FLAG-YopT(C139S) plasmids. After overnight incubation, cells were lysed in Tris-buffered saline containing 1% Triton X-114 (Sigma) and lysates were cleared by centrifugation. Cleared lysates were partitioned into aqueous and detergent (aliphatic) phases by incubation at 37°C for 5 min, and each phase was subjected to IP with anti-myc or anti-HA resin. Precipitated proteins were eluted by boiling in sample buffer and analyzed using sodium dodecyl sulfate-polyacrylamide gel electrophoresis and Western blotting.

Statistical analysis. Data were analyzed using GraphPad Prism software, and *P* values were generated using a two-tailed unpaired *t* test.

RESULTS

RhoG localization to nascent *Yersinia*-containing phagosomes requires a high-affinity invasin-β1 integrin interaction. Recruitment of RhoG to *Y. pseudotuberculosis*-containing phagosomes in COS1 cells transiently transfected with EGFP-RhoG was investigated. In order to assay RhoG recruitment to nascent phagosomes in the absence of any interference from Yops, a plasmid-cured *Y. pseudotuberculosis* strain that encodes no Yops [YPIII(P^-)] was used. This strain promotes uptake through invasin interaction with β1 integrins (1, 57). Efficient recruitment of both wild-type and constitutively active RhoG to nascent phagosomes was observed (Fig. 1A, wt and G12V). The dominant-negative form of RhoG failed to localize to nascent phagosomes (Fig. 1A, T17N) in contrast to previous observations with Rac1 (38).

In order to determine if high-affinity bacterial adhesion is required for RhoG recruitment to nascent phagosomes, a mutant invasin allele (*invD911A*) that binds β1 integrins, but with significantly lower affinity than wild-type invasin, was used (29). The *Y. pseudotuberculosis invD911A* strain was incubated with cells expressing GFP-tagged RhoG, and localization was visualized as described above, using Rac1 as a positive control (57). No significant RhoG recruitment was observed after challenge with the *Y. pseudotuberculosis invD911A* strain (Fig. 1B, compare wt and D911A), which is similar to what was observed with Rac1 (Fig. 1B), indicating that tight invasin-β1 integrin interaction is required for efficient RhoG recruitment. Variations in expression levels as a cause for differences in localization phenotypes were ruled out because robust expression of both RhoG and Rac1 mutant forms was observed (data not shown).

RhoG inactivation significantly reduces efficiency of invasin-mediated phagocytosis. The requirement for RhoG during invasin-mediated uptake was examined next. COS1 cells transiently expressing wild-type and dominant-negative RhoG [RhoG (T17N)], were challenged with *Y. pseudotuberculosis* YPIII(P^-), and the uptake efficiency was determined (see Materials and Methods). The uptake efficiency in cells expressing RhoG(T17N) was significantly reduced to levels similar to those observed after challenging cells expressing dominant-negative Rac1 [Rac1(T17N)] (1, 57) (Fig. 2A). Also, expres-

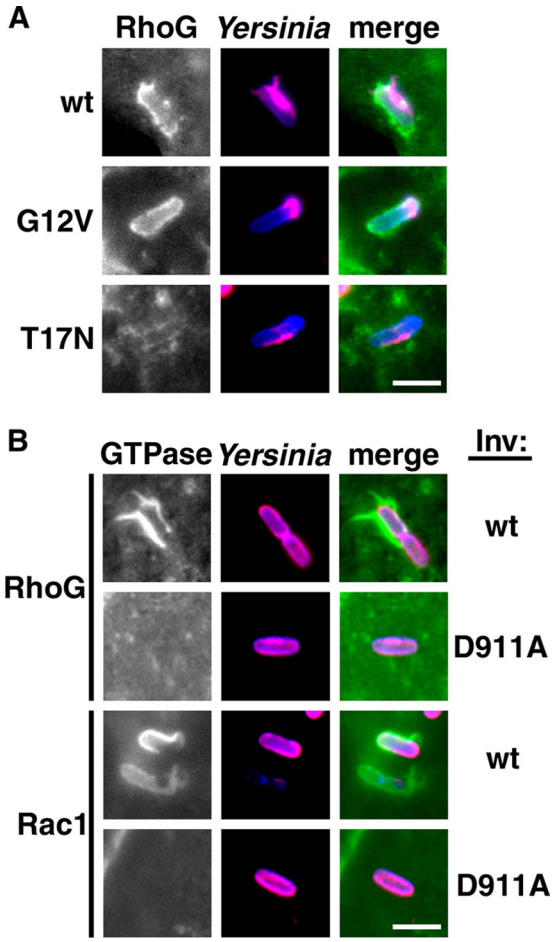

FIG. 1. RhoG localizes to nascent *Yersinia*-containing phagosomes in an invasin-dependent manner. (A) Wild-type and constitutively active but not dominant-negative RhoG proteins localize to nascent phagosomes. COS1 cells expressing wild-type (wt), constitutively active (G12V), or dominant-negative (T17N) RhoG constructs (GFP fusions) were incubated briefly (~20 min) with *Y. pseudotuberculosis* YPIII(P^-). Localization at nascent phagosomes was visualized by fluorescence microscopy (see Materials and Methods). Extracellular portions of bacteria appear pink/red, and intracellular portions appear blue. (B) Robust RhoG localization to nascent phagosomes is dependent upon high-affinity β1 integrin ligation. COS1 cells expressing the wild-type alleles of RhoG and Rac1 (GFP fusions) were incubated with *Y. pseudotuberculosis* encoding either wild-type or D911A invasin (Inv), which binds to β1 integrins at a much lower affinity than the wild type. Localization of GFP fusions at the nascent phagosome was visualized as described for panel A. Scale bars (applicable to all images within the respective panels) = 3 μm.

sion of constitutively active RhoG or Rac1 had no effect, either negative or positive, on uptake levels compared to wild-type levels (data not shown). These data indicate that RhoG activity is crucial for efficient bacterial uptake.

The T17N dominant-negative mutant protein in Ras superfamily GTPases functions by tightly binding to endogenous GEFs that normally activate the GTPase (16), thus preventing the activation of endogenous GTPase pools. If the binding of the dominant-negative protein to GEFs is promiscuous or if the dominant-negative protein titrates proteins that normally act downstream of Rac1 activation, then the observed defect could be unrelated to a role for RhoG signaling. To reduce the chance of artifactual observations and to confer more specificity on the observed uptake defect phenotypes, we used RNAi to deplete RhoG and Rac1. Plasmids encoding shRNAs targeting RhoG and Rac1, as well as a control nontargeting shRNA, were transfected into HeLa cells. The efficiency of transcript depletion was quantified using quantitative RT-PCR after 48 h. This method showed that levels of RhoG and Rac1 transcripts were significantly reduced after shRNA treatment (Fig. 2B). Approximately 48 h posttransfection, cells were incubated with *Y. pseudotuberculosis* YPIII(P^-) and uptake was measured microscopically. Uptake in RhoG- and Rac1-depleted cells was significantly reduced compared with that in mock-depleted cells (Fig. 2C). Potential "off-target" effects are unlikely since RhoG depletion did not affect Rac1 transcript levels and vice versa (Fig. 2B) and because multiple shRNA depleting constructs produced identical phenotypes (data not shown). Interestingly, it appears that, at least in the case of invasin-mediated uptake, there is no significant difference in phenotype between dominant-negative versus RNAi inactivation of RhoG.

Development of a FRET-based biosensor to monitor RhoG activation. To investigate whether or not the recruited RhoG is activated, we took advantage of FRET to develop a biosensor that detects the activation state of RhoG (Fig. 3A). No such biosensor has been reported, as RhoG activation has been assayed either by IP experiments (27) or by relocalization of an effector (42). While useful for examining activity in bulk, IP methods give no information about localized GTPase activity, and relocalization methods do not directly measure activity.

The newly developed FRET-based biosensor described here relies on the fact that RhoG interacts with the effector molecule ELMO only when activated (27) (Fig. 3A; see Materials and Methods for a detailed description of the biosensor constructs). The N-terminal 362 amino acids of ELMO have been shown to be sufficient for this GTP-dependent interaction; active Rac1, Cdc42, and RhoA do not show any detectable interaction with ELMO (27). The biosensor is encoded on two plasmids and comprises RhoG fused to the C terminus of monomeric CFP (mCFP) (mCFP-RhoG) and ELMO amino acids 1 to 362 [ELMO(AA1-362)] fused to the N terminus of mYFP (ELMO-mYFP). Upon GTP-dependent interaction of RhoG with ELMO, fused CFP and YFP are brought into close proximity whereby energy emitted by CFP could be absorbed by YFP and subsequently generate a FRET signal (Fig. 3A).

The nucleotide dependence of the system was evaluated first. mCFP-RhoG and ELMO-mYFP constructions were expressed in COS1 cells, and FRET was measured microscopically (see Materials and Methods). Wild-type RhoG generated detectable levels of FRET signal (Fig. 3B; quantified in panel E). RhoG(G12V) is insensitive to GAP inactivation and thus is constitutively GTP associated. As expected, the FRET signal generated by this mutant was higher than that observed with wild-type RhoG (Fig. 3C; quantified in panel E). The dominant-negative mutant RhoG(T17N), which is defective in GTP loading, generated significantly lower FRET signals, as did the effector binding mutants RhoG(F37A) and RhoG(Y40C) (Fig. 3D; quantified in panels E and F). These results indicate that the RhoG-ELMO biosensor is sensitive to changes in the nu-

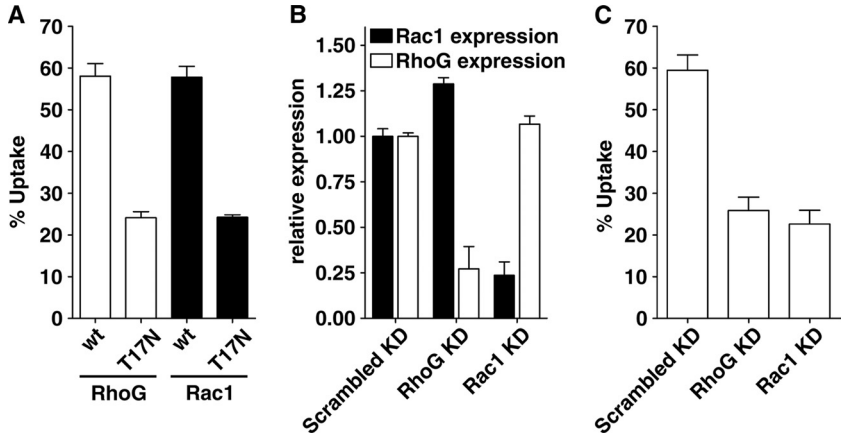

FIG. 2. RhoG inactivation leads to reduced uptake. (A) Expression of dominant-negative RhoG significantly reduces bacterial uptake efficiency. COS1 cells were transfected with either wild-type (wt) or dominant-negative (T17N) GTPase constructs overnight. Transfected cells were then incubated with *Y. pseudotuberculosis* YPIII(P^-), and uptake was quantified microscopically as described in Materials and Methods. *P* was <0.0001 for the wt versus T17N both RhoG and Rac1 (B) RNAi-mediated depletion of RhoG. HeLa cells were transfected with plasmids encoding hairpin sequences (shRNA) targeting either RhoG or Rac1. A nontargeting shRNA (scrambled) was used as the control. Quantitative RT-PCR was used to quantify the extent of depletion by each shRNA after 48 h. Data were first normalized to GAPDH transcript levels in each sample and are presented here as fractions of expression relative to the control (scrambled). KD, knockdown. For RhoG and Rac1 expression, *P* was <0.0001 (scrambled KD versus RhoG KD and scrambled KD versus Rac1 KD, respectively). (C) RhoG depletion leads to significantly lower uptake efficiency. HeLa cells were depleted of the indicated GTPases for ~48 h. Cells were then incubated with *Y. pseudotuberculosis* YPIII(P^-), and uptake was quantified as described above. For scrambled KD versus RhoG KD and Rac1 KD, *P* was <0.0001.

cleotide binding state of RhoG and can function to report the activation state of RhoG.

Localized RhoG activation in response to *Yersinia* binding to host cells. Using the previously mentioned IP method, RhoG activation in response to *Y. enterocolitica* binding has been demonstrated (42). The FRET biosensor was used to assess if the activation of RhoG in response to invasin-mediated signaling was localized. This approach was similar to one used previously to analyze localized Rac1 activation at the site of bacterial attachment (57). COS1 cells expressing the RhoG biosensor constructs were challenged with *Y. pseudotuberculosis* YPIII(P^-), fixed, and processed for fluorescence imaging. Elevation in FRET signal at the nascent phagosome indicated robust RhoG activation at the site of bacterial contact (Fig. 4A). Quantitation of FRET also showed a dramatic increase in local RhoG activity at nascent phagosomes (Fig. 4B). As expected, Rac1 was also activated at the site of attachment (Fig. 4C).

RhoG is inactivated by *Y. pseudotuberculosis* YopE. *Y. pseudotuberculosis* translocates several proteins into the host cell cytosol via its T3SS. One such protein, YopE, is a GAP that has been shown to inactivate Rac1, RhoA, and Cdc42 (3). Inactivation of Rho GTPases by YopE inhibits phagocytosis, which serves to maintain extracellular localization of the pathogen. The RhoG FRET biosensor was used to evaluate inactivation of RhoG by YopE. COS1 cells expressing the FRET biosensor were challenged with YP17 (YPIII Δ*yopE* Δ*yopH*) and YP17/pYopE for 2 h, fixed, and imaged for FRET. Interestingly, lower FRET signals were detected in cells that were incubated with YopE-expressing bacteria (Fig. 5A and B), suggesting that RhoG is inactivated by YopE. For quantification, cells were challenged briefly (~30 min) with YP17 and YP17/pYopE and fixed and the extent of RhoG activation at the site of bacterial attachment was quantified as described above. The duration of bacterial challenge was minimized because prolonged exposure to YopE causes cell rounding (note cell shape in Fig. 5A and B), which may lead to significant cell loss and microscopic images that cannot be readily quantified. We found that the amount of RhoG-ELMO FRET at nascent phagosomes was significantly reduced in the presence of YopE (Fig. 5C). This result was consistent with (i) RhoG being inactivated by the action of *Y. pseudotuberculosis* YopE and (ii) previous observations of *Y. enterocolitica* YopE's RhoG GAP activity (42). Interestingly, cytoplasmic levels of RhoG-ELMO FRET (i.e., activation at regions without bound bacteria) remained relatively unchanged (Fig. 5D). This lack of cytoplasmic inactivation may be due to the short period of infection used in the assay, or cytoplasmic pools of RhoG may be resistant to the activity of YopE.

RhoG is mislocalized by *Y. pseudotuberculosis* YopT. YopT is a prenylcysteine endoprotease that is translocated by *Yersinia* into host cells (46, 51). *Y. pseudotuberculosis* YopT mislocalizes Rac1, Cdc42, and RhoA by cleaving the C-terminal lipid moiety, thereby removing the membrane-targeting signal. We first examined the mislocalization of GTPases at the whole-cell level by incubating cells expressing EGFP-tagged RhoG and Rac1 with YopT-expressing and control bacteria and examining changes in GTPase localization. In the absence of YopT, RhoG was found to localize to a perinuclear focus as well as the cytosol (Fig. 6A, −YopT). This intricate localization was dramatically disrupted upon incubation with YopT-expressing bacteria (Fig. 6A, +YopT). The majority of EGFP-Rac1 was relocated to the nucleus in response to YopT-expressing bacteria (Fig. 6B), as previously described (56, 57).

We assayed targeting and cleavage of RhoG by microscopic observation of GTPase localization to nascent phagosomes containing bacteria with and without YopT. EGFP-RhoG-expressing cells were challenged with bacteria expressing YopT,

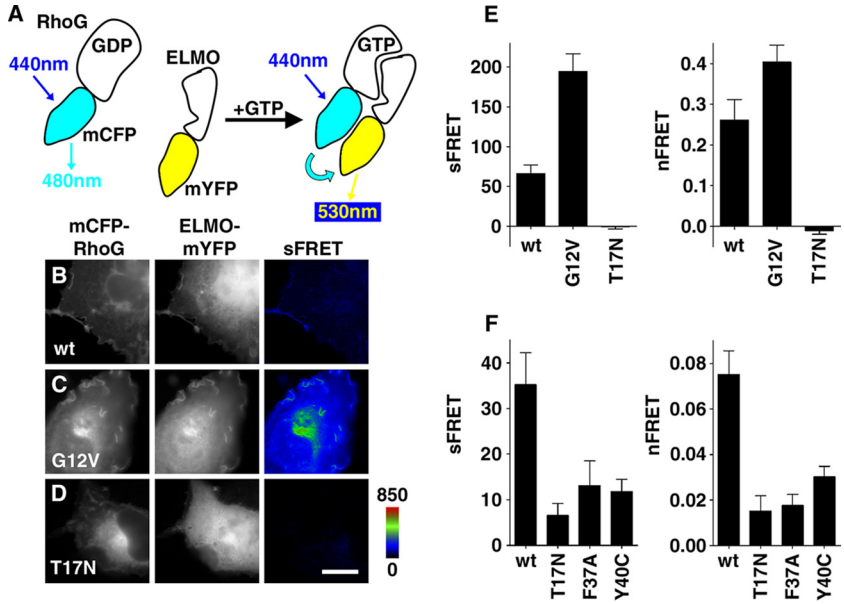

FIG. 3. Development of a FRET-based RhoG activation biosensor. (A) Schematic of the RhoG activation biosensor. The biosensor is made from two constructs: mCFP-RhoG and ELMO(AA1-362)–mYFP. Upon GTP loading RhoG-ELMO interaction brings the two fluorescent proteins into close proximity, allowing transfer of energy from CFP to YFP. This energy transfer is visualized microscopically. (B to D) RhoG activation in COS1 cells expressing the RhoG FRET biosensor. COS1 cells were transfected with mCFP fusions of wild-type (wt) (B), constitutively active (G12V) (C), or dominant-negative (T17N) (D) RhoG along with ELMO-mYFP. sFRET images were calculated as described in Materials and Methods. Scale bar (applicable to all images) = 15 μm. (E) RhoG-ELMO FRET quantification shows a higher signal using constitutively active RhoG and a lower signal using dominant-negative RhoG. FRET was quantified at multiple ROIs in multiple cells as described in Materials and Methods and is presented as sFRET and nFRET. For sFRET, P was <0.0001 for wt versus RhoG(G12V) and 0.0007 for wt versus RhoG(T17N); for nFRET, P was <0.05 for wt versus RhoG(G12V) and 0.0024 for wt versus RhoG(T17N). (F) RhoG effector binding mutants [RhoG(F37A) and RhoG(Y40C)] display lower FRET readouts than the wild type. Quantification was carried out as described above. For sFRET, P was 0.0005 for the wt versus RhoG(T17N), 0.0172 for the wt versus RhoG(F37A), and 0.0023 for the wt versus RhoG(Y40C); for nFRET, P was <0.0001 for the wt versus RhoG(T17N) and RhoG(F37A) and 0.0002 for the wt versus RhoG(Y40C).

and nascent phagosomes were scored for GTPase localization. This assay showed less RhoG localization on nascent phagosomes in the presence of YopT (Fig. 7A; quantified in panel B), consistent with YopT cleavage of the RhoG C-terminal prenyl moiety. This targeting was specific, because a GTPase known not to be targeted by YopT, Arf6, was not removed from nascent phagosomes (Fig. 7A and B). Rac1 was included in this assay as a known target of YopT cleavage (Fig. 7A and B).

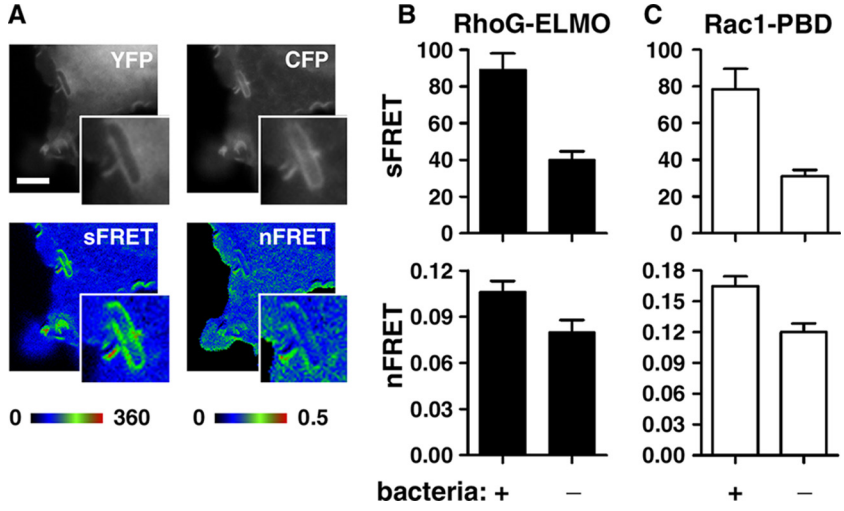

FIG. 4. Localized RhoG activation at nascent phagosomes. (A) *Yersinia* binding activates RhoG. COS1 cells expressing the RhoG FRET biosensor were incubated with *Yersinia* YPIII(P$^-$), fixed, and imaged as described for Fig. 3. Scale bar (applicable to all images except insets) = 5 μm. (B and C) Quantitative increase in FRET signal in response to bacterial binding. RhoG-ELMO- and Rac1-p21 binding domain-expressing cells were imaged for FRET. sFRET and nFRET at ROIs with (+) or without (−) bound bacteria are presented. nFRET was calculated by normalizing sFRET values for donor and acceptor concentrations at each ROI. At least 12 independent ROIs were quantified in each analysis group. RhoG sFRET, $P < 0.0001$; RhoG nFRET, $P = 0.0185$; Rac1 sFRET, $P = 0.0004$; Rac1 nFRET, $P = 0.0014$.

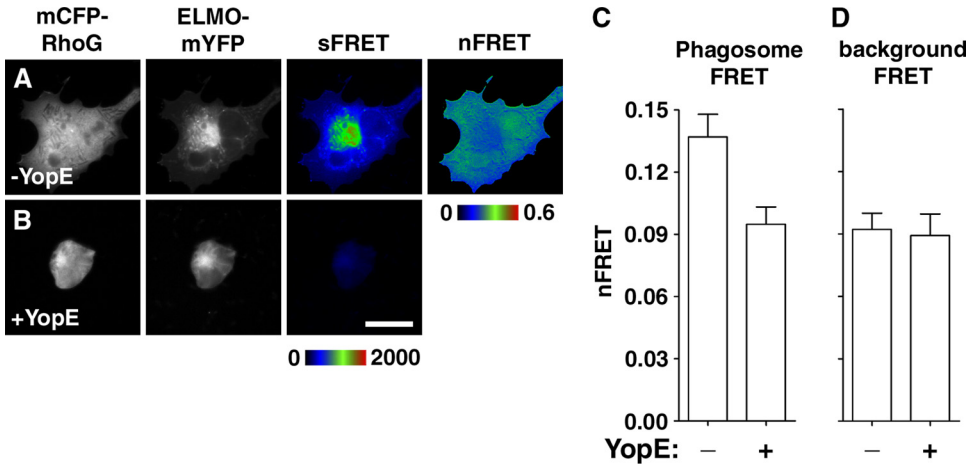

FIG. 5. *Y. pseudotuberculosis* YopE inactivates RhoG. (A and B) YopE inactivation of cellular pools of RhoG. COS1 cells expressing the RhoG FRET biosensor were incubated for 2 h with a *Y. pseudotuberculosis* strain with an inducible plasmid encoding YopE (see Materials and Methods for details). A strain carrying the empty plasmid was used as the control. sFRET and nFRET images were calculated as described in Materials and Methods. Scale bar (applicable to all images) = 20 μm. (C) YopE causes localized RhoG inactivation. COS1 cells expressing the RhoG FRET biosensor were incubated briefly (~30 min) with *Y. pseudotuberculosis* strains as for panels A and B, and FRET was quantified at the site of bacterial attachment. Normalized FRET figures from these sites are presented. *P*, 0.0053. (D) YopE-mediated RhoG inactivation is a localized event. RhoG activation at sites without bacterial attachment (background FRET) was quantified as described above. *P*, 0.883.

RhoG cleavage by YopT was also assayed biochemically. Cleared lysates from 293T cells expressing constitutively active RhoG and YopT(wt) or YopT(C139S), a catalytically inactive mutant (46), were fractionated into aqueous (nonprenylated) and aliphatic (prenylated) fractions using Triton X-114 (22, 46). In order to minimize potential artifacts caused by GTPase inactivation and subsequent Rho guanine nucleotide dissociation inhibitor (RhoGDI) association, which may interfere with YopT targeting and cleavage, constitutively active forms of GTPases were used in this assay. In cells expressing YopT(wt), RhoG was excluded from the detergent-associated fraction after Triton X-114 partitioning, providing further support for the notion that YopT cleaves RhoG (Fig. 7C, lanes wt; quantified in panel D). This depletion was dependent upon the catalytic activity of YopT, as the partitioning was unaffected in YopT(C139S)-expressing cells (Fig. 7C and D, lanes CS). Once again, a noncleavable GTPase (Arf6) did not display any altered partitioning behavior, and the known YopT substrate (Rac1) was efficiently cleaved (Fig. 7C and D). These results strongly suggest that YopT does indeed cleave RhoG. Furthermore, as there was no significant shift in RhoG electrophoretic mobility in the Triton X-114 partitioning assay, it is likely that the cleavage site in RhoG is indeed at the extreme C terminus of the protein, as described previously for Rac1, Cdc42, and RhoA (47).

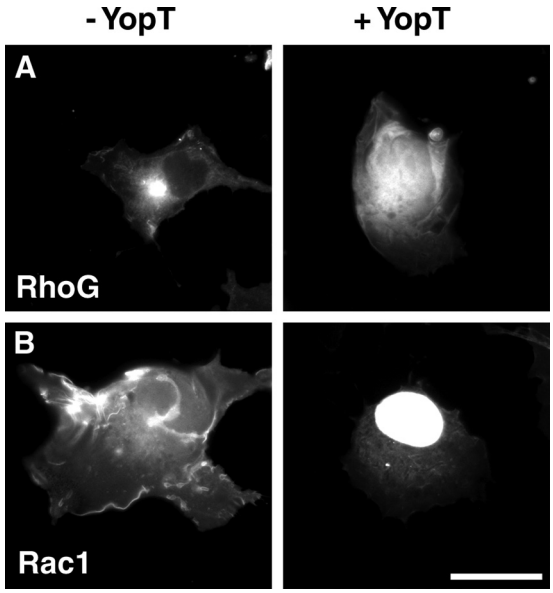

FIG. 6. Global Rho GTPase mislocalization by *Y. pseudotuberculosis* YopT. (A) YopT disrupts intricate subcellular localization of RhoG. COS1 cells expressing EGFP-tagged constitutively active RhoG were incubated with YP17 (−YopT) or YP17/pYopT (+YopT) for 30 min, fixed, and processed for fluorescence imaging. (B) YopT mislocalizes Rac1 to the nucleus. Scale bar (applicable to all images) = 30 μm.

Assessment of RhoG and Rac1 interplay during invasin-mediated uptake. The relationship between RhoG and Rac1 signaling is unclear. Some groups have shown that RhoG activates Rac1 and Cdc42 (termed linear signaling) (17, 27), whereas others have found that RhoG signals independently of other Rho GTPases (termed parallel signaling) (41, 55). Invasin binding activates both RhoG and Rac1, so we decided to investigate if linear signaling from RhoG to Rac1 was required for invasin-mediated uptake. To this end, we took advantage of the Rho GAP activity of YopE. YopE was used to inactivate both endogenous RhoG and Rac1 in the cell, leading to significantly lower bacterial uptake efficiency (Fig. 8A, plasmid). Constitutively active Rho GTPases are insensitive to Rho GAP inactivation, so COS1 cells expressing either RhoG(G12V) or Rac1(G12V) were challenged with YopE-expressing bacteria and uptake was quantified. Uptake of YopE-expressing bacteria was restored when either of the constitutively active GTPases was expressed (Fig. 8A, RhoG G12V and Rac1 G12V),

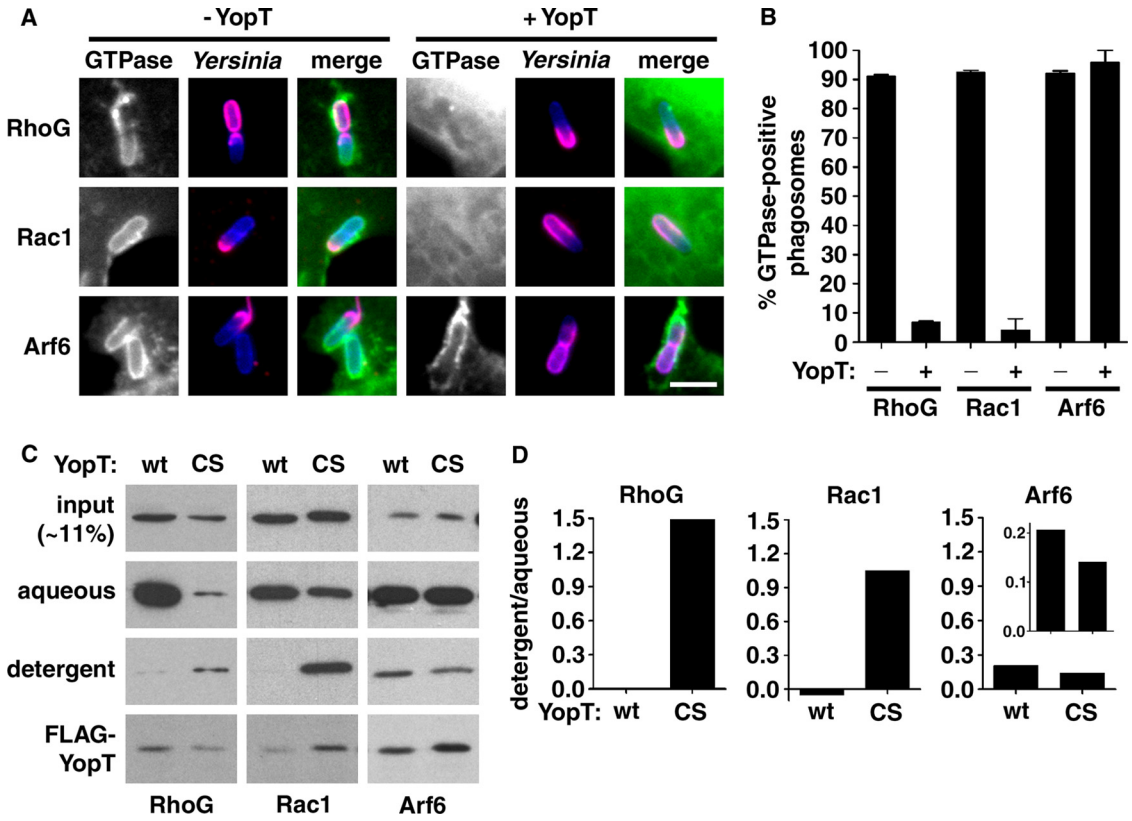

FIG. 7. *Y. pseudotuberculosis* YopT mislocalizes RhoG. (A) YopT removes RhoG from nascent phagosomes. COS1 cells expressing EGFP-RhoG, EGFP-Rac1, and Arf6-HA were incubated with control and YopT-expressing strains of *Y. pseudotuberculosis*. Cells were fixed and stained to visualize GTPases and bacteria (see Materials and Methods). Scale bar (applicable to all images) = 3 μm. (B) Quantification of phenotype described for panel A. Fifty individual phagosomes were scored for GTPase presence in each of three independent samples. *P* values were calculated by comparing conditions with and without YopT. RhoG, $P < 0.0001$; Rac1, $P = 0.0021$; Arf6, $P = 0.464$. (C) Alteration in RhoG prenylation in YopT-expressing cells. 293T cells, transfected with constitutively active RhoG, Rac1, or Arf6 along with YopT(wt) (wt) or YopT(C139S) (CS), were lysed using Triton X-114 and partitioned into aqueous and aliphatic (detergent) fractions. Each fraction was analyzed for the presence of GTPase by IP and Western blotting. Input samples were analyzed for the presence of the indicated GTPases and FLAG-YopT by blotting. (D) Quantification of Triton X-114 fractionation. Band intensities in panel C were quantified by densitometry, and the quantities of each GTPase present in aqueous and detergent fractions were normalized to input quantities. A ratio of normalized detergent to normalized aqueous GTPase is presented. Arf6 quantities were regraphed with an alternate *y*-axis scale and are presented as an inset.

indicating that either GTPase could be used to control events associated with uptake in the absence of the other.

The suppression assay with constitutively active RhoG assumes equivalent toxin delivery in the presence or absence of constitutively active RhoG. Rho GTPase activity has been shown to influence T3SS function (34), as Mejia et al. found that inactivation of Rho GTPases leads to decreased Yop translocation efficiency. However, the effect of constitutively active RhoG expression upon toxin delivery is unknown, so we assayed the translocation efficiency of YopE with or without constitutively active RhoG. Transfected COS1 cells were challenged with wild-type *Y. pseudotuberculosis* (translocation competent) as well as an isogenic *yopB* mutant (translocation defective). Eukaryotic cells were lysed, and the extent of translocation was determined using a detergent fractionation method followed by Western blotting (see Materials and Methods). Immunodetection of YopE showed that similar quantities of YopE were translocated regardless of RhoG(G12V) expression status (Fig. 8B), which indicates that expression of constitutively active RhoG does not alter the efficiency of Yop delivery in *Y. pseudotuberculosis*.

We used a secondary assay to test for the presence of parallel signaling. COS1 cells were cotransfected with either dominant-negative RhoG and constitutively active Rac1 or constitutively active RhoG and dominant-negative Rac1. These cells were challenged with YPIII(P^-), and invasin-mediated uptake was quantified. Single transfections with dominant-negative and constitutively active GTPases were used as controls. As expected, dominant-negative RhoG and Rac1 significantly reduced uptake whereas constitutively active RhoG and Rac1 did not (Fig. 8C). Notably, expression of constitutively active RhoG restored uptake to cells expressing dominant-negative Rac1, suggesting that RhoG signaling can occur independently of the Rac1 activation state (Fig. 8C). Evidence presented here indicates that RhoG can bypass the requirement for Rac1 during invasin-mediated uptake.

Both assays used to examine the issue of dependent versus independent signaling provide evidence for independent sig-

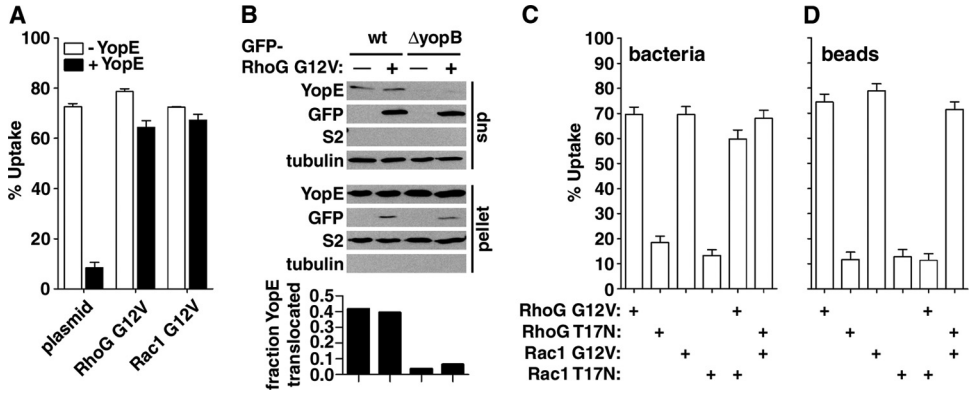

FIG. 8. RhoG and Rac1 signal in parallel during *Yersinia* uptake but signal linearly during large-particle uptake. (A) Endogenous GTPase inactivation by YopE could be suppressed by expression of constitutively active RhoG. Cells expressing constitutively active RhoG or Rac1 [RhoG(G12V) or Rac1(G12V)] or control cells (plasmid) were challenged with control or YopE-expressing *Yersinia*. Uptake was quantified as described in Materials and Methods. In the presence of YopE, *P* was <0.0001 for the control cells versus cells expressing RhoG(G12V) or Rac1(G12V). (B) Expression of constitutively active RhoG does not affect efficiency of Yop translocation by *Y. pseudotuberculosis*. COS1 cells were transfected with RhoG(G12V) or a control plasmid. Cells were then incubated with *Y. pseudotuberculosis* YPIII(P^+) (wt) or the isogenic *yopB* deletion mutant (Δ*yopB*). After incubation with bacteria, host cells were lysed using Nonidet P-40 and fractionated into detergent-soluble (sup) and detergent-insoluble (pellet) fractions by centrifugation. Both fractions were analyzed by Western blotting. The percentage of translocated YopE was calculated by performing densitometry to quantify blots. (C and D) The bacterial uptake defect due to RhoG inactivation could be suppressed by expression of constitutively active Rac1 and vice versa, but large-particle uptake could not. COS1 cells were transfected with constitutively active (G12V) or dominant-negative (T17N) forms of Rac1 and RhoG, either individually or in combination, as indicated. Transfected cells were then incubated with *Yersinia* YPIII(P^-) or large (4.1-μm) invasin-coated beads, and uptake was quantified as described in Materials and Methods. *P* values are as follows: wt RhoG or Rac1 versus T17N mutant, 0.0001 (C and D); RhoG(T17N) and Rac1(T17N) versus RhoG(G12V)/Rac1(T17N) and Rac1(G12V)/RhoG(T17N), <0.0001 (C); RhoG(T17N) versus RhoG(T17N)/Rac1(G12V), <0.0001 (D); Rac1(T17N) versus RhoG(G12V)/Rac1(T17N), 0.7235 (D).

naling during uptake, which contradicts published reports of the role of RhoG during phagocytosis (11). deBakker et al. found, using plastic beads as phagocytic particles, that expression of constitutively active RhoG could not suppress the uptake defect seen with dominant-negative Rac1. Invasin is sufficient for phagocytic uptake, so we quantified uptake of large (4.1-μm) latex beads coated with purified invasin. In contrast to what was found for bacterial internalization, the defect in the uptake of 4.1-μm beads in cells expressing dominant-negative Rac1 could not be suppressed by expression of constitutively active RhoG (Fig. 8D). Furthermore, constitutively active Rac1 could bypass the defect caused by dominant-negative RhoG (Fig. 8D). The latter results are in accordance with previous observations and indicate that large-particle uptake requires a linear pathway of signaling from RhoG to Rac1. Therefore, it appears that the nature and/or surface area involved in phagocytosis determines if RhoG can mediate uptake under conditions in which there are limiting levels of functional Rac1.

DISCUSSION

In this work we demonstrated that the Rho GTPase RhoG is targeted by three *Yersinia pseudotuberculosis* virulence factors. In the absence of Yop expression, RhoG was recruited to the site of bacterial attachment as a result of a high-affinity invasin-β1 integrin interaction (Fig. 1), and RhoG inactivation resulted in reduced bacterial uptake efficiency (Fig. 2). A novel FRET biosensor (Fig. 3) was used to observe accumulation of activated RhoG at sites of bacterial attachment (Fig. 4). The translocated toxins YopE (a Rho GAP) and YopT (a prenylcysteine endoprotease) both targeted RhoG: YopE inactivated RhoG and YopT cleaved and mislocalized RhoG (Fig. 5, 6, and 7). The various methods of RhoG manipulation by *Y. pseudotuberculosis* are depicted in Fig. 9.

In evaluating the effect of RhoG inactivation upon invasin-mediated signaling, we used a dominant-negative RhoG allele (encoding the T17N mutation) as well as RNAi-mediated depletion. In our system, both inactivating approaches yielded similar results, causing a defect in invasin-mediated uptake (Fig. 2). In other systems dominant-negative mutants have been shown to generate potentially artifactual findings (21, 37). Patel and Galan (37) have shown that dominant-negative Cdc42 interferes with *Salmonella enterica*-induced ruffle formation, whereas Cdc42 RNAi does not. Similarly, Hakeda-Suzuki et al. (21) found that inactivating mutations in *Drosophila melanogaster* Rac1 do not affect the establishment of cell polarity, whereas dominant-negative mutants do. The system used here—invasin-β1 integrin-mediated signaling through RhoG and Rac1—seems insensitive to such confounding results.

Differences between Rac1 and RhoG recruitment to nascent phagosomes are notable. Patel et al. (38) observed that Rac1, in the absence of activating signals, is recruited to nascent Fc receptor phagosomes, concluding that Rac1 activation occurs after recruitment to phagosomes. In contrast, our observations indicate that inactive RhoG is not recruited to nascent phagosomes (Fig. 1), suggesting that the mechanisms for recruitment and activation may differ between the two highly similar GTPases. It is possible that different factors mediate RhoGDI dissociation for each GTPase, especially since each interacts with a different RhoGDI isoform. Rac1 shows specificity for RhoGDI-1, while RhoG is sequestered by RhoGDI-3 (5, 36).

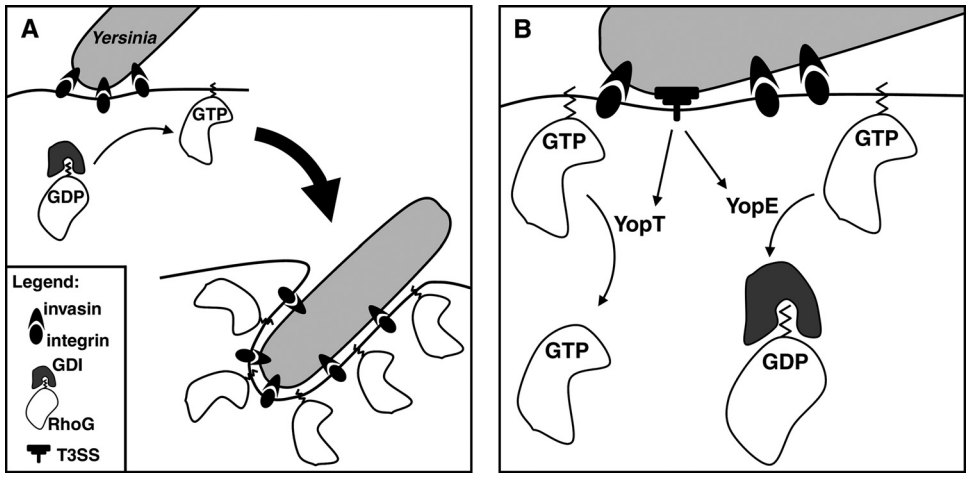

FIG. 9. Model of RhoG manipulation by *Yersinia pseudotuberculosis*. (A) RhoG is activated in response to invasin-mediated signaling. When there is no expression of antiphagocytic factors, invasin binding to β1 integrin activates RhoG. Activated (GTP-bound) RhoG, liberated from RhoGDI, localizes to membranous structures through its C-terminal prenyl moiety, where effector association occurs. Invasin-mediated Rho GTPase activation may be somewhat redundant, as both RhoG and Rac1 are activated, leading to efficient internalization of the bacterium. (B) RhoG is inactivated and mislocalized by YopE and YopT, respectively. Under conditions in which Yops are translocated into the cytosol, both YopE and YopT misregulate RhoG. YopE, a Rho GAP, inactivates RhoG, and YopT, a prenylcysteine endoprotease, most likely cleaves RhoG, thereby removing the C-terminal lipid moiety that mediates membrane localization. YopT cleavage leads to the accumulation of a cytosol-localized pool that is resistant to sequestration by RhoGDI. This pool may represent a previously unappreciated signaling niche for RhoG.

Alternatively, the difference in recruitment may be due to variations in each of the PBRs. That is, both GTPases are liberated from their respective RhoGDIs by a similar mechanism but localize differently in the absence of activation due to differences in the number of basic residues in the PBR, since the number of C-terminal basic residues has been shown to influence subcellular localization (59).

The fate of YopT-cleaved RhoG is unclear. In the case of Rac1, cleavage exposes a nuclear localization signal, leading to the accumulation of activated Rac1 in the nucleus (35, 57), but no such signal exists in RhoG. Differences between YopT-mediated RhoG and Rac1 mislocalization are depicted in Fig. 6. Triton X-114 fractionation of cells coexpressing RhoG and YopT (Fig. 7) showed an increase in the aqueous form of RhoG, which most likely localizes to the cytosol. This aberrantly localized pool of RhoG, which most likely lacks C-terminal prenylation and thus cannot be sequestered by RhoGDI, may be a new signaling niche for RhoG. Furthermore, the cleaved pool of RhoG is most likely not inactivated by YopE, since evidence exists for cytosolic Rac1 not being susceptible to YopE inactivation (57). Exposure of the cytosolic compartment to active RhoG may lead to a number of atypical outcomes, ranging from altered immune signaling to altered cytoskeletal rearrangement events. Triton X-114 fractionation shows a marked accumulation of YopT-cleaved RhoG in the aqueous fraction, which is absent in cleaved Rac1 (Fig. 7C; compare aqueous fractions in RhoG and Rac1 panels). This difference is most likely due to the fact that Triton X-114 does not disrupt the nucleus, which contains a significant fraction of YopT-cleaved Rac1 (Fig. 6).

We have used RhoG-ELMO FRET to show RhoG inactivation in the presence of YopE, but this does not directly demonstrate that YopE is a RhoG GAP. Roppenser et al., however, have shown that purified *Y. enterocolitica* YopE acts as a GAP for RhoG (42), so it is likely that the *Y. pseudotuberculosis* YopE used in this study is also a RhoG GAP, especially since *Y. enterocolitica* YopE and *Y. pseudotuberculosis* YopE are 94% identical at the primary protein sequence level.

We have observed that Rac1 and RhoG are able to signal redundantly during invasin-mediated uptake of bacteria, but RhoG and Rac1 functions do not overlap. Inactivation of RhoG by YopE or mislocalization by YopT may be a way of expanding the targeted Rho GTPase repertoire by *Y. pseudotuberculosis*. Inactivating Rac1 is crucial for antiphagocytosis, but it may be insufficient to cripple the antibacterial activity of immune cells such as neutrophils. By targeting RhoG, a factor that is required for the generation of ROS by neutrophils, *Y. pseudotuberculosis* drastically interferes with an important arm of the host immune defense. Infection of RhoG-deficient mice with *Y. pseudotuberculosis* may shed light on the importance of RhoG in the context of a fully intact immune system, especially since $RhoG^{-/-}$ mice show no apparent defects in immune system development (53). In addition, RhoG is uniquely localized compared with other Rho GTPases. The active form of RhoG has been shown to localize to the plasma membrane as well as to perinuclear structures that may be of Golgi or endoplasmic reticulum nature (5, 41). This is in contrast to active Rac1, which localizes almost exclusively to the plasma membrane. By inhibiting both Rho GTPases, *Y. pseudotuberculosis* also increases the range of compartments it is able to target. YopE displays a perinuclear localization pattern when expressed in CHO cells (28), so targeting GTPases that reside in that vicinity is entirely possible. The significance of such differential compartment targeting is not clear but may contribute to successful establishment and progression of disease.

We investigated the interplay between RhoG and Rac1 signaling during phagocytic uptake (Fig. 8) and found evidence for both linear and parallel signaling depending on the size of the ingested particle. Both GTPases are activated in response to bacterial binding, but inactivation of only one does not affect

uptake efficiency in the presence of a constitutively active form of either GTPase. In contrast, large-particle uptake efficiency is significantly decreased when either GTPase is inactivated, but Rac1 inactivation cannot be overcome by expression of constitutively active RhoG, indicating that large-particle uptake requires signaling from RhoG to Rac1. Active Rac1, on the other hand, can bypass the loss of RhoG function in this case. Observed differences between results described here and previous work may be attributed to assays used. Most previous conclusions have been based on observed changes in cell morphology (17) and assays directly looking at GTPase activation (27, 41) or effector/GEF interaction (55), while we investigated the issue using a functional phagocytosis assay. This assay demonstrates that the requirement for a particular GTPase is partly determined by the nature of the signaling event being assayed.

Roppenser et al. recently reported that RhoG is targeted by the related organism *Yersinia enterocolitica* via invasin and YopE (42). We demonstrate here that *Y. pseudotuberculosis* YopE and invasin behave similarly. In addition, we demonstrate that *Y. pseudotuberculosis* YopT effectively cleaves RhoG (Fig. 7). Roppenser et al. conclude that, in response to bacterial attachment, Rac1 signaling depends on RhoG. Although we believe this to be correct, we find that if the surface of the phagocytic particle is sufficiently small, activated RhoG can bypass a defect in Rac1 signaling. This may be a consequence of the activation of a small pool of Rac1 or of the direct replacement of Rac1 by RhoG and activation of downstream effectors that may normally associate with Rac1 signaling. Clearly, as the surface area of the phagosome is increased, such bypass cannot occur.

Pathogenic *Yersinia* species encode sophisticated systems to dampen the host response and proliferate successfully. Misregulation of RhoG appears to be yet another clever adaptation by these organisms that has not been uncovered previously, and precise ramifications of this misregulation remain to be investigated. Our study has shed light on RhoG's unique nature among GTPases that are misregulated by *Y. pseudotuberculosis*. Despite a high degree of primary sequence similarity to such GTPases as Rac1, RhoG's distinctive subcellular localization and crucial role in proper neutrophil function make it stand out as a novel target of pathogenic *Yersinia*.

ACKNOWLEDGMENTS

We thank Elizabeth Creasey, Matthew Heidtman, Gregory Crimmins, Alexander Engsminger, Tamara O'Connor, Molly Bergman, Eva Haenssler, Irene Newton, and Aisling Dugan for critical review of the text; James Bliska (Stony Brook University), Joan Mecsas (Tufts University School of Medicine), Hironori Katoh (Kyoto University), and Crislyn D'Souza-Schorey (University of Notre Dame) for supplying plasmids and bacterial strains; and Kathleen Riendeau for technical assistance with preparation of the manuscript.

This work was supported by the Howard Hughes Medical Institute (HHMI), by award R37AI23538 and training grant 5T32AI007422 from the National Institute of Allergy and Infectious Diseases, and Program Project Award grant P30DK34928 from the National Institute of Diabetes and Digestive and Kidney Diseases. R. R. Isberg is an Investigator of HHMI.

REFERENCES

1. **Alrutz, M. A., A. Srivastava, K. W. Wong, C. D'Souza-Schorey, M. Tang, L. E. Ch'Ng, S. B. Snapper, and R. R. Isberg.** 2001. Efficient uptake of *Yersinia pseudotuberculosis* via integrin receptors involves a Rac1-Arp 2/3 pathway that bypasses N-WASP function. Mol. Microbiol. **42:**689–703.
2. **Autenrieth, I. B., V. Kempf, T. Sprinz, S. Preger, and A. Schnell.** 1996. Defense mechanisms in Peyer's patches and mesenteric lymph nodes against *Yersinia enterocolitica* involve integrins and cytokines. Infect. Immun. **64:**1357–1368.
3. **Black, D. S., and J. B. Bliska.** 2000. The RhoGAP activity of the *Yersinia pseudotuberculosis* cytotoxin YopE is required for antiphagocytic function and virulence. Mol. Microbiol. **37:**515–527.
4. **Bolin, I., L. Norlander, and H. Wolf-Watz.** 1982. Temperature-inducible outer membrane protein of *Yersinia pseudotuberculosis* and *Yersinia enterocolitica* is associated with the virulence plasmid. Infect. Immun. **37:**506–512.
5. **Brunet, N., A. Morin, and B. Olofsson.** 2002. RhoGDI-3 regulates RhoG and targets this protein to the Golgi complex through its unique N-terminal domain. Traffic **3:**342–357.
6. **Cerione, R. A., and Y. Zheng.** 1996. The Dbl family of oncogenes. Curr. Opin. Cell Biol. **8:**216–222.
7. **Condliffe, A. M., L. M. Webb, G. J. Ferguson, K. Davidson, M. Turner, E. Vigorito, M. Manifava, E. R. Chilvers, L. R. Stephens, and P. T. Hawkins.** 2006. RhoG regulates the neutrophil NADPH oxidase. J. Immunol. **176:**5314–5320.
8. **Conlan, J. W.** 1997. Critical roles of neutrophils in host defense against experimental systemic infections of mice by *Listeria monocytogenes*, *Salmonella typhimurium*, and *Yersinia enterocolitica*. Infect. Immun. **65:**630–635.
9. **Cornelis, G. R.** 2002. The *Yersinia* Ysc-Yop 'type III' weaponry. Nat. Rev. Mol. Cell Biol. **3:**742–752.
10. **Davis, A. J., and J. Mecsas.** 2007. Mutations in the *Yersinia pseudotuberculosis* type III secretion system needle protein, YscF, that specifically abrogate effector translocation into host cells. J. Bacteriol. **189:**83–97.
11. **deBakker, C. D., L. B. Haney, J. M. Kinchen, C. Grimsley, M. Lu, D. Klingele, P. K. Hsu, B. K. Chou, L. C. Cheng, A. Blangy, J. Sondek, M. O. Hengartner, Y. C. Wu, and K. S. Ravichandran.** 2004. Phagocytosis of apoptotic cells is regulated by a UNC-73/TRIO-MIG-2/RhoG signaling module and armadillo repeats of CED-12/ELMO. Curr. Biol. **14:**2208–2216.
12. **DerMardirossian, C., and G. M. Bokoch.** 2005. GDIs: central regulatory molecules in Rho GTPase activation. Trends Cell Biol. **15:**356–363.
13. **Dersch, P., and R. R. Isberg.** 1999. A region of the *Yersinia pseudotuberculosis* invasin protein enhances integrin-mediated uptake into mammalian cells and promotes self-association. EMBO J. **18:**1199–1213.
14. **Dovas, A., and J. R. Couchman.** 2005. RhoGDI: multiple functions in the regulation of Rho family GTPase activities. Biochem. J. **390:**1–9.
15. **D'Souza-Schorey, C., R. L. Boshans, M. McDonough, P. D. Stahl, and L. Van Aelst.** 1997. A role for POR1, a Rac1-interacting protein, in ARF6-mediated cytoskeletal rearrangements. EMBO J. **16:**5445–5454.
16. **Feig, L. A.** 1999. Tools of the trade: use of dominant-inhibitory mutants of Ras-family GTPases. Nat. Cell Biol. **1:**E25–E27.
17. **Gauthier-Rouviere, C., E. Vignal, M. Meriane, P. Roux, P. Montcourier, and P. Fort.** 1998. RhoG GTPase controls a pathway that independently activates Rac1 and Cdc42Hs. Mol. Biol. Cell **9:**1379–1394.
18. **Gemski, P., J. R. Lazere, T. Casey, and J. A. Wohlhieter.** 1980. Presence of a virulence-associated plasmid in *Yersinia pseudotuberculosis*. Infect. Immun. **28:**1044–1047.
19. **Gey, G. O., W. D. Coffman, and M. T. Kubicek.** 1952. Tissue culture studies of the proliferative capacity of cervical carcinoma and normal epithelium. Cancer Res. **12:**264–265.
20. **Gluzman, Y.** 1981. SV40-transformed simian cells support the replication of early SV40 mutants. Cell **23:**175–182.
21. **Hakeda-Suzuki, S., J. Ng, J. Tzu, G. Dietzl, Y. Sun, M. Harms, T. Nardine, L. Luo, and B. J. Dickson.** 2002. Rac function and regulation during *Drosophila* development. Nature **416:**438–442.
22. **Hancock, J. F.** 1995. Prenylation and palmitoylation analysis. Methods Enzymol. **255:**237–245.
23. **Hynes, R. O.** 2002. Integrins: bidirectional, allosteric signaling machines. Cell **110:**673–687.
24. **Isberg, R. R., and P. Barnes.** 2001. Subversion of integrins by enteropathogenic *Yersinia*. J. Cell Sci. **114:**21–28.
25. **Isberg, R. R., and J. M. Leong.** 1990. Multiple beta 1 chain integrins are receptors for invasin, a protein that promotes bacterial penetration into mammalian cells. Cell **60:**861–871.
26. **Jaffe, A. B., and A. Hall.** 2005. Rho GTPases: biochemistry and biology. Annu. Rev. Cell Dev. Biol. **21:**247–269.
27. **Katoh, H., and M. Negishi.** 2003. RhoG activates Rac1 by direct interaction with the Dock180-binding protein Elmo. Nature **424:**461–464.
28. **Krall, R., Y. Zhang, and J. T. Barbieri.** 2004. Intracellular membrane localization of *Pseudomonas* ExoS and *Yersinia* YopE in mammalian cells. J. Biol. Chem. **279:**2747–2753.
29. **Leong, J. M., P. E. Morrissey, A. Marra, and R. R. Isberg.** 1995. An aspartate residue of the *Yersinia pseudotuberculosis* invasin protein that is critical for integrin binding. EMBO J. **14:**422–431.
30. **Logsdon, L. K., and J. Mecsas.** 2003. Requirement of the *Yersinia pseudotuberculosis* effectors YopH and YopE in colonization and persistence in intestinal and lymph tissues. Infect. Immun. **71:**4595–4607.
31. **Marketon, M. M., R. W. DePaolo, K. L. DeBord, B. Jabri, and O. Schnee-**

wind. 2005. Plague bacteria target immune cells during infection. Science **309:**1739–1741.
32. **Marra, A., and R. R. Isberg.** 1997. Invasin-dependent and invasin-independent pathways for translocation of *Yersinia pseudotuberculosis* across the Peyer's patch intestinal epithelium. Infect. Immun. **65:**3412–3421.
33. **Matsumoto, H., and G. M. Young.** 2009. Translocated effectors of *Yersinia*. Curr. Opin. Microbiol. **12:**94–100.
34. **Mejia, E., J. B. Bliska, and G. I. Viboud.** 2008. *Yersinia* controls type III effector delivery into host cells by modulating Rho activity. PLoS Pathog. **4:**e3.
35. **Michaelson, D., W. Abidi, D. Guardavaccaro, M. Zhou, I. Ahearn, M. Pagano, and M. R. Philips.** 2008. Rac1 accumulates in the nucleus during the G_2 phase of the cell cycle and promotes cell division. J. Cell Biol. **181:**485–496.
36. **Michaelson, D., J. Silletti, G. Murphy, P. D'Eustachio, M. Rush, and M. R. Philips.** 2001. Differential localization of Rho GTPases in live cells: regulation by hypervariable regions and RhoGDI binding. J. Cell Biol. **152:**111–126.
37. **Patel, J. C., and J. E. Galan.** 2006. Differential activation and function of Rho GTPases during *Salmonella*-host cell interactions. J. Cell Biol. **175:**453–463.
38. **Patel, J. C., A. Hall, and E. Caron.** 2002. Vav regulates activation of Rac but not Cdc42 during FcγR-mediated phagocytosis. Mol. Biol. Cell **13:**1215–1226.
39. **Pepe, J. C., M. R. Wachtel, E. Wagar, and V. L. Miller.** 1995. Pathogenesis of defined invasion mutants of *Yersinia enterocolitica* in a BALB/c mouse model of infection. Infect. Immun. **63:**4837–4848.
40. **Portnoy, D. A., H. Wolf-Watz, I. Bolin, A. B. Beeder, and S. Falkow.** 1984. Characterization of common virulence plasmids in *Yersinia* species and their role in the expression of outer membrane proteins. Infect. Immun. **43:**108–114.
41. **Prieto-Sanchez, R. M., and X. R. Bustelo.** 2003. Structural basis for the signaling specificity of RhoG and Rac1 GTPases. J. Biol. Chem. **278:**37916–37925.
42. **Roppenser, B., A. Roder, M. Hentschke, K. Ruckdeschel, and M. Aepfelbacher.** 2009. *Yersinia enterocolitica* differentially modulates RhoG activity in host cells. J. Cell Sci. **122:**696–705.
43. **Rossman, K. L., C. J. Der, and J. Sondek.** 2005. GEF means go: turning on RHO GTPases with guanine nucleotide-exchange factors. Nat. Rev. Mol. Cell Biol. **6:**167–180.
44. **Sebti, S. M., and C. J. Der.** 2003. Opinion: searching for the elusive targets of farnesyltransferase inhibitors. Nat. Rev. Cancer **3:**945–951.
45. **Shao, F.** 2008. Biochemical functions of *Yersinia* type III effectors. Curr. Opin. Microbiol. **11:**21–29.
46. **Shao, F., P. M. Merritt, Z. Bao, R. W. Innes, and J. E. Dixon.** 2002. A *Yersinia* effector and a *Pseudomonas* avirulence protein define a family of cysteine proteases functioning in bacterial pathogenesis. Cell **109:**575–588.
47. **Shao, F., P. O. Vacratsis, Z. Bao, K. E. Bowers, C. A. Fierke, and J. E. Dixon.** 2003. Biochemical characterization of the *Yersinia* YopT protease: cleavage site and recognition elements in Rho GTPases. Proc. Natl. Acad. Sci. USA **100:**904–909.
48. **Spinner, J. L., J. A. Cundiff, and S. D. Kobayashi.** 2008. *Yersinia pestis* type III secretion system-dependent inhibition of human polymorphonuclear leukocyte function. Infect. Immun. **76:**3754–3760.
49. **Tcherkezian, J., and N. Lamarche-Vane.** 2007. Current knowledge of the large RhoGAP family of proteins. Biol. Cell **99:**67–86.
50. **Viboud, G. I., and J. B. Bliska.** 2001. A bacterial type III secretion system inhibits actin polymerization to prevent pore formation in host cell membranes. EMBO J. **20:**5373–5382.
51. **Viboud, G. I., and J. B. Bliska.** 2005. *Yersinia* outer proteins: role in modulation of host cell signaling responses and pathogenesis. Annu. Rev. Microbiol. **59:**69–89.
52. **Viboud, G. I., E. Mejia, and J. B. Bliska.** 2006. Comparison of YopE and YopT activities in counteracting host signalling responses to *Yersinia pseudotuberculosis* infection. Cell. Microbiol. **8:**1504–1515.
53. **Vigorito, E., S. Bell, B. J. Hebeis, H. Reynolds, S. McAdam, P. C. Emson, A. McKenzie, and M. Turner.** 2004. Immunological function in mice lacking the Rac-related GTPase RhoG. Mol. Cell. Biol. **24:**719–729.
54. **Wennerberg, K., and C. J. Der.** 2004. Rho-family GTPases: it's not only Rac and Rho (and I like it). J. Cell Sci. **117:**1301–1312.
55. **Wennerberg, K., S. M. Ellerbroek, R. Y. Liu, A. E. Karnoub, K. Burridge, and C. J. Der.** 2002. RhoG signals in parallel with Rac1 and Cdc42. J. Biol. Chem. **277:**47810–47817.
56. **Wong, K. W., and R. R. Isberg.** 2003. Arf6 and phosphoinositol-4-phosphate-5-kinase activities permit bypass of the Rac1 requirement for beta1 integrin-mediated bacterial uptake. J. Exp. Med. **198:**603–614.
57. **Wong, K. W., and R. R. Isberg.** 2005. *Yersinia pseudotuberculosis* spatially controls activation and misregulation of host cell Rac1. PLoS Pathog. **1:**e16.
58. **Wong, K. W., S. Mohammadi, and R. R. Isberg.** 2008. The polybasic region of Rac1 modulates bacterial uptake independently of self-association and membrane targeting. J. Biol. Chem. **283:**35954–35965.
59. **Yeung, T., G. E. Gilbert, J. Shi, J. Silvius, A. Kapus, and S. Grinstein.** 2008. Membrane phosphatidylserine regulates surface charge and protein localization. Science **319:**210–213.

Editor: J. B. Bliska